Second Virial Coefficient of Isotactic Oligo- and Poly(methyl methacrylate)s. Effects of Chain Stiffness and Chain Ends

Masanao Kamijo, Fumiaki Abe, Yoshiyuki Einaga, and Hiromi Yamakawa*

Department of Polymer Chemistry, Kyoto University, Kyoto 606-01, Japan

Received December 27, 1994; Revised Manuscript Received March 27, 1995[⊗]

ABSTRACT: The second virial coefficient A_2 was determined for isotactic poly(methyl methacrylate) (i-PMMA) over a wide range of weight-average molecular weight M_w from 7.89×10^2 to 1.93×10^6 in acetone at 25.0 °C, for $M_w \geq 1.55 \times 10^5$ in chloroform at 25.0 °C and in nitroethane at 30.0 °C, and for $M_w = 6.88 \times 10^5$ in acetonitrile at 35.0, 45.0, and 55.0 °C. (Some of the data had already been obtained in the previous work.) It is shown that the observed dependence of A_2 on M_w in the oligomer region may be quantitatively explained by the Yamakawa theory that takes account of the effect of chain ends. The values of the effective excess binary-cluster integrals β_1 and β_2 associated with the chain end beads are then found to be 66 and 360 Å^3, respectively, in acetone at 25.0 °C by taking the repeat unit as a single bead. The analysis shows that the effect of chain ends remains even for relatively large M_w in the good solvent as in the cases of atactic polystyrene (a-PS) and atactic poly(methyl methacrylate) (a-PMMA). The results for the true interpenetration function Ψ in A_2 without the effect of chain ends indicate that the two-parameter theory breaks down completely, as found previously for a-PS and a-PMMA; the observed Ψ as a function of the cubed gyration-radius expansion factor α_S^3 depends separately on M_w and on the reduced excluded-volume strength λB. It is found that the values of Ψ for i-PMMA are appreciably smaller than thsoe for a-PMMA in the same solvent, i.e., for the same value of the binary-cluster integral β, while the former values almost coincide with the latter for the same λB. The Yamakawa theory that takes account of the effects of chain stiffness and local chain conformation on the basis of the helical wormlike chain may explain satisfactorily the observed behavior of Ψ and also the remarkable difference in it between i-PMMA and a-PMMA, the effects appearing in Ψ through both λB and the mean-square radius of gyration $\langle S^2 \rangle$.

Introduction

In previous papers of this series,[1–3] we have investigated effects of chain stiffness and chain ends on the second virial coefficient A_2 and the interpenetration function Ψ appearing in it for atactic oligo- and polystyrenes (a-PS) and atactic oligo- and poly(methyl methacrylate)s (a-PMMA). The results have confirmed the validity of the Yamakawa theory[4] of A_2 that takes account of these effects on the basis of the helical wormlike (HW) chain model.[5,6] It predicts that the chain stiffness has a significant effect on Ψ even for such large molecular weight M that the ratio of the unperturbed mean-square radius of gyration $\langle S^2 \rangle_0$ to M already reaches its coil-limiting value independent of M and also that the effect of chain ends on A_2 becomes appreciable for relatively small M. The observed behavior of A_2 as a function of M and of Ψ as a function of the cubed gyration-radius expansion factor α_S^3 can be satisfactorily explained by this theory. Specifically, both theoretically and experimentally, Ψ is not a universal function of α_S^3 but its change with α_S^3 depends separately also on M and on the excluded-volume strength (or solvent power) B, indicating that the two-parameter theory[7] breaks down completely. It has also been shown that the observed remarkable difference in Ψ between a-PS and a-PMMA may be well explained by the theory as arising from the large differences in chain stiffness and local chain conformation between these two polymers.

In the present work, we make a similar study of A_2 and Ψ for isotactic poly(methyl methacrylate) (i-PMMA) with the fraction of racemic diads $f_r \simeq 0.01$ over a wide range of M including the oligomer region. We have already investigated extensively dilute solution properties of i-PMMA in the Θ state.[8–11] It has then been shown that they may be explained consistently by the HW theory, and thus the values of the HW model parameters for i-PMMA have already been determined. The results show that there are significant differences in chain stiffness and local chain conformation between the i- and a-PMMAs. Very recently, we have also made a study of α_S and the viscosity-radius expansion factor α_η for i-PMMA[12] to confirm that the quasi-two-parameter scheme is valid for both α_S and α_η, irrespective of the large differences in chain stiffness, local chain conformation, and solvent condition, for i-PMMA as well as for a-PMMA,[13] a-PS,[14–16] and polyisobutylene.[15] That is, α_S and α_η for them become functions only of the scaled excluded-volume parameter $\tilde{z}$ defined in the Yamakawa–Stockmayer–Shimada (YSS) theory[17–19] for the perturbed HW chain with excluded volume.

Now the interesting finding in the previous study[12] of α_S and α_η is that the values of the binary-cluster integral β between beads (segments) for the i- and a-PMMAs in the same solvent (acetone and chloroform) are almost identical with each other, indicating that β is independent of the stereochemical structure of the polymer chain. Thus the main purpose of this paper is to examine the effects of chain stiffness and local chain conformation on Ψ for the two PMMAs with the same excluded-volume interaction (β) between beads. For this purpose, we determine A_2 and Ψ for i-PMMA in the same good solvents, i.e., acetone and chloroform at 25.0 °C and also nitroethane at 30.0 °C, as used in the previous study[3] of A_2 for a-PMMA. We may then investigate differences in the behavior of Ψ between them, which may be considered to arise solely from the above effects. (We also determine Ψ for i-PMMA in

[⊗] Abstract published in *Advance ACS Abstracts,* May 1, 1995.

0024-9297/95/2228-4159$09.00/0

Table 1. Values of M_w, x_w, and M_w/M_n for Isotactic Oligo- and Poly(methyl methacrylate)s

sample	M_w	x_w	M_w/M_n
iOM7[a]	7.89×10^2	7.31	1.01
iOM10[b]	1.01×10^3	9.52	1.02
iOM16	1.56×10^3	15.0	1.02
iOM18	1.79×10^3	17.3	1.10
iOM31	3.12×10^3	30.6	1.07
iOM71	7.07×10^3	70.1	1.05
iMM1	1.07×10^4	106	1.05
iMM3	3.06×10^4	305	1.06
iMMc6	5.89×10^4	588	1.08
iMMc10	9.87×10^4	986	1.08
iMMc16	1.55×10^5	1550	1.08
iMMc30	3.13×10^5	3130	1.08
iMMc40	3.80×10^5	3800	1.06
iMMc70	6.88×10^5	6880	1.06
iMMc90	9.46×10^5	9460	1.09
iMMc190	1.93×10^6	19300	1.09

[a] M_w of iOM7 had been determined from GPC.[8] [b] M_ws of iOM10 through iMMc190 had been determined from LS in acetonitrile at 28.0 °C (Θ),[8,10,12] except for iOM16 (present work).

acetonitrile above Θ to examine its behavior near $\alpha_S^3 = 1$.)

Experimental Section

Materials. Most of the i-PMMA samples used in this work are the same as those used in the previous studies of the mean-square radii of gyration $\langle S^2\rangle_\Theta$ and $\langle S^2\rangle$,[8,12] the scattering function $P(k)$,[9] the intrinsic viscosities $[\eta]_\Theta$ and $[\eta]$,[10,12] the translational diffusion coefficient D_Θ,[10] and the mean-square optical anisotropy $\langle\Gamma^2\rangle$,[11] i.e., the fractions separated by preparative gel permeation chromatography (GPC) or fractional precipitation from the original samples prepared by living anionic polymerization or from the commercial sample 9011-14-7 from Scientific Polymer Products, Inc. In this work, however, one additional sample was also obtained by preparative GPC from the former. The synthesized samples have a *tert*-butyl group at the initiating chain end and a hydrogen atom at the other end. All the samples have a fixed stereochemical composition ($f_r \simeq 0.01$) independent of M.

The values of the weight-average molecular weight M_w, the weight-average degree of polymerization x_w, and the ratio of M_w to the number-average molecular weight M_n are listed in Table 1. The sample iOM16 is the additional one, and its M_w was determined from light scattering (LS) measurements in acetone at 25.0 °C. The values of M_w/M_n indicate that the molecular weight distributions of all the samples are sufficiently narrow for the present purpose.

The solvents acetone, chloroform, nitroethane, and acetonitrile used for LS measurements were purified according to standard procedures.

Light Scattering. LS measurements were carried out to determine A_2 (and also $\langle S^2\rangle$ and M_w) for the i-PMMA samples with $M_w \le 1.55 \times 10^5$ in acetone at 25.0 °C, for the sample iMMc16 in chloroform at 25.0 °C, and for the samples with $M_w \ge 1.55 \times 10^5$ in nitroethane at 30.0 °C. Measurements were also made to determine A_2 and $\langle S^2\rangle$ for the sample iMMc70 in acetonitrile at temperatures higher than Θ (28.0 °C). A Fica 50 light scattering photometer was used for all the measurements with vertically polarized incident light of wavelength 436 nm. For a calibration of the apparatus, the intensity of light scattered from pure benzene was measured at 25.0 °C at a scattering angle of 90°, where the Rayleigh ratio $R_{Uu}(90°)$ of pure benzene was taken as 46.5×10^{-6} cm^{-1}. The depolarization ratio ϱ_u of pure benzene at 25.0 °C was determined to be 0.41 ± 0.01 by the method of Rubingh and Yu.[20]

The conventional method was used for solutions of the samples with $M_w > 10^3$, while the new procedure previously[21] presented was applied to the oligomer sample iOM7 with $M_w = 7.89 \times 10^2$, since the concentration dependence of the density scattering R_d and the optical constant K have significant effects on the determination of A_2 (and also of M_w) for such small M_w.

In the analysis of the data obtained by the conventional method we employed the Berry square-root plot[22] as usual. For the low-molecular-weight samples with $10^3 < M_w < 10^4$, the measurements were made in the range of the polymer mass concentration c from 7×10^{-3} to 1.3×10^{-1} g/cm^3, keeping the excess scattering intensities at least 80% of that from the solvent acetone. The accuracies were then within ±0.5%. The correction for the anisotropic scattering was then applied to the solutions of the samples with $10^3 < M_w \lesssim 3.1 \times 10^3$ (as usual by the use of eq 1 of ref 21).

In order to determine A_2 by the latter method,[21] we measured the reduced total intensity R^*_{Uv} of unpolarized scattered light for vertically polarized incident light, the depolarization ratio ϱ_u, the ratio of the isothermal compressibility of a given solution to that of the solvent $\kappa_T/\kappa_{T,0}$, and the refractive index increment $(\partial\tilde{n}/\partial c)_{T,p}$ for the oligomer solutions, and also the first two quantities for the solvents. The values of the refractive index $\tilde{n}$ at finite concentrations c, which were required to calculate K, were calculated with the values of $(\partial\tilde{n}/\partial c)_{T,p}$ for the sample iOM7, as described in the Results. The measurements of R^*_{Uv} were carried out at scattering angles θ ranging from 37.5 to 142.5°, and the mean of the values obtained at different θ was adopted as its value, since it must be independent of θ for oligomers. The values of ϱ_u were obtained by the same method as employed in the calibration of the apparatus. The analysis of the LS data obtained was also made by using the Berry square-root plot.

The most concentrated solutions of each sample were prepared by continuous stirring at room temperature for ca. 1 day in acetone, in chloroform, and in nitroethane and at ca. 50 °C for 4 days in acetonitrile. They were optically purified by filtration through a Teflon membrane of pore size 0.45 or 0.10 μm. The solutions of lower concentrations were obtained by successive dilution. The polymer mass concentrations c were calculated from the weight fractions with the densities of the solutions. The densities of the solvents and solutions were measured with a pycnometer of the Lipkin–Davison type.

The values of $\partial\tilde{n}/\partial c$ at 436 nm for i-PMMA are 0.138_0 and 0.065_0 cm^3/g in acetone at 25.0 °C for $M_w \gtrsim 3.0 \times 10^5$ and in chloroform at 25.0 °C for $M_w \gtrsim 3.0 \times 10^4$, respectively.[8,12] The value determined for i-PMMA in nitroethane at 30.0 °C with a Shimadzu differential refractometer was 0.100_5 cm^3/g for $M_w \gtrsim 10^4$. For each oligomer sample with $M_w \le 3.12 \times 10^3$ in acetone at 25.0 °C, $\partial\tilde{n}/\partial c$ was determined as a function of c by the use of the same refractometer.

Isothermal Compressibility. Isothermal compressibility measurements were carried out to determine $\kappa_T/\kappa_{T,0}$ for the oligomer sample iOM7 in acetone at 25.0 °C. The apparatus and the method of measurements are the same as those described in the previous paper.[2] The ratio $\kappa_T/\kappa_{T,0}$ was determined as a function of c and pressure p. The pressure p was varied from 1 to ca. 50 atm. This ratio was found to be independent of p within experimental error at any concentration c in this range of p, and therefore we adopted the mean of the values obtained at various pressures as its value at 1 atm.

Results

Light Scattering from the Oligomer iOM7 in Acetone. It has been found that $\kappa_T/\kappa_{T,0}$ for the sample iOM7 in acetone at 25.0 °C decreases linearly with increasing c as in the case of a-PMMA.[3] (The values of $\kappa_T/\kappa_{T,0}$ obtained are 0.950 and 0.913 at $c = 0.050\ 97$ and 0.1433 g/cm^3, respectively.) The results may then be represented by the equation linear in c

$$\kappa_T/\kappa_{T,0} = 1 + kc \qquad (1)$$

with $k = -0.73$ cm^3/g for $c \lesssim 0.15$ g/cm^3. (Note that the value of k is identical with that for a-PMMA in acetone at 25.0 °C.)

The values of $(\partial\tilde{n}/\partial c)_{T,p}$ at 436 nm determined to evaluate $\tilde{n}$ and K at finite concentrations c have been found to be independent of c for $c \lesssim 0.15$ g/cm^3 for iOM7

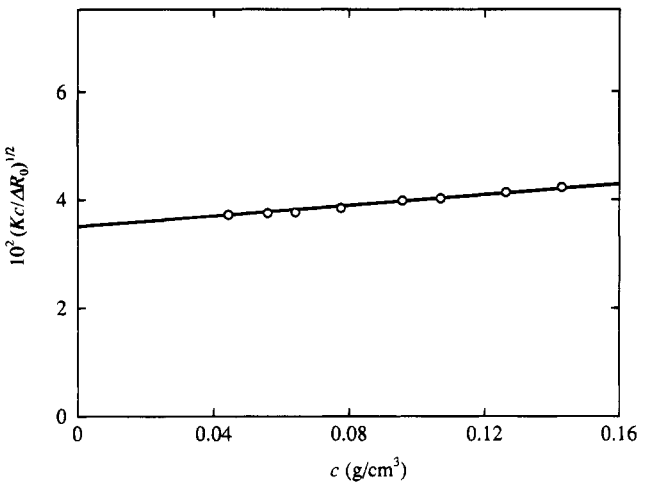

Figure 1. Plots of $(Kc/\Delta R_0)^{1/2}$ against c for the i-PMMA sample iOM7 in acetone at 25.0 °C.

in acetone at 25.0 °C, its constant value being 0.120_5 cm^3/g. Thus, for the solution of iOM7, the values of $\tilde{n}$ at c in the range of c above may be obtained from the equation

$$\tilde{n} = \tilde{n}_0 + (\partial\tilde{n}/\partial c)_{T,p}c \qquad (2)$$

with $\tilde{n}_0 = 1.3647$ for pure acetone at 25.0 °C and the above value of $(\partial\tilde{n}/\partial c)_{T,p}$.

Figure 1 shows the Berry square-root plots of the excess Rayleigh ratio ΔR_0 at $\theta = 0$ against c for the i-PMMA sample iOM7 in acetone at 25.0 °C. It is seen that the data points follow a straight line in the range of c studied, from which M_w and the light scattering second virial coefficient A_2' can be determined accurately. The value of A_2' thus obtained may be equated to that of the (osmotic) second virial coefficient A_2 as in the case of a-PMMA.[3]

Similar results for the Berry square-root plots have also been obtained for the other samples with higher molecular weights in acetone and in the other solvents studied by the conventional method, and their A_2 and M_w have been determined with sufficient accuracy as usual, so that we do not show the plots explicitly. We note that it has already been reported[3] that the values of A_2 determined from the Berry square-root plots agree well with those from the Bawn plots.[23,24] We also note that for iOM10, iOM16, iOM18, and iOM31 in acetone at 25.0 °C, the values of $\partial\tilde{n}/\partial c$ were 0.124, 0.128, 0.131, and 0.137 cm^3/g, respectively, and for higher-molecular-weight samples, it is 0.138_0 cm^3/g, as given above.

Second Virial Coefficient. The values of A_2 determined from LS measurements in acetone at 25.0 °C, in chloroform at 25.0 °C, in nitroethane at 30.0 °C, and in acetonitrile at three temperatures above Θ are summarized in Tables 2–5, respectively, along with those of M_w and $\langle S^2\rangle^{1/2}$. Tables 2 and 3 also include the unpublished data for A_2 for the samples with $M_w \geq 3.16 \times 10^5$ in acetone at 25.0 °C and in chloroform at 25.0 °C, respectively, which had already been determined in ref 12.

Figure 2 shows double-logarithmic plots of A_2 against M_w for i-PMMA in the three good solvents acetone at 25.0 °C (unfilled circles), chloroform at 25.0 °C (top-half-filled circles), and nitroethane at 30.0 °C (bottom-half-filled circles). It also includes the previous results[3] for a-PMMA in the same solvents (triangles), for comparison. The heavy and light solid curves connect the data points smoothly (the latter for a-PMMA). It is seen that

Table 2. Results of LS Measurements on Isotactic Oligo- and Poly(methyl methacrylate)s in Acetone at 25.0 °C

sample	$10^{-4}M_w$	10^4A_2, (cm^3 mol)/g^2	$\langle S^2\rangle^{1/2}$, Å[a]
iOM7	0.0814	17.2	(6.40)[b]
iOM10	0.105	14.1	7.64
iOM16	0.156	9.41	
iOM18	0.183	8.60	
iOM31	0.304	7.03	16.0
iOM71	0.727	4.03	25.1
iMM1	1.05	4.14	31.4
iMM3	3.09	2.85	55.6
iMMc6	5.98	2.36	
iMMc10	9.83	2.22	
iMMc16	15.4	2.15	139
iMMc30[c]	31.6	1.80	203
iMMc40	37.9	1.75	226
iMMc70	68.6	1.50	314
iMMc90	97.8	1.46	383
iMMc190	197	1.23	574

[a] The data for $\langle S^2\rangle^{1/2}$ have been reproduced with permission from ref 12 except for iMMc16 (present work). [b] The value (in parentheses) in acetonitrile at 28.0 °C (Θ).[8] [c] The data for iMMc30 through iMMc190 in acetone have been reproduced from ref 12 with permission except for A_2, the values of which were not reported there, although already determined.

Table 3. Results of LS Measurements on Isotactic Poly(methyl methacrylate) in Chloroform at 25.0 °C

sample	$10^{-4}M_w$	10^4A_2, (cm^3 mol)/g^2	$\langle S^2\rangle^{1/2}$, Å
iMMc16	16.0	6.92	172
iMMc30[a]	31.6	6.12	264
iMMc40	38.5	5.57	296
iMMc70	69.4	4.91	421
iMMc90	97.8	4.39	515
iMMc190	197	3.80	778

[a] The data for iMMc30 through iMMc190 have been reproduced from ref 12 with permission except for A_2, the values of which were not reported there, although already determined.

Table 4. Results of LS Measurements on Isotactic Poly(methyl methacrylate) in Nitroethane at 30.0 °C

sample	$10^{-4}M_w$	10^4A_2, (cm^3 mol)/g^2	$\langle S^2\rangle^{1/2}$, Å
iMMc16	15.3	4.33	153
iMMc30	30.8	3.66	226
iMMc40	37.3	3.47	255
iMMc70	67.7	3.03	356
iMMc90	98.6	2.64	444
iMMc190	192	2.33	662

Table 5. Results of LS Measurements on the Sample iMMc70 in Acetonitrile at 55.0, 45.0, and 35.0 °C

temp, °C	10^4A_2, (cm^2 mol)/g^2	$\langle S^2\rangle^{1/2}$, Å
55.0	0.57_7	277
45.0	0.40_0	266
35.0	0.20_1	262

the values of A_2 for i-PMMA in chloroform and in nitroethane are ca. 20% larger than the corresponding values for a-PMMA, while the plots for them have almost the same slope. On the other hand, the data points for i-PMMA in acetone are seen to be very close to those for a-PMMA in the same solvent except in the range of $M_w \lesssim 2 \times 10^3$, for which A_2 is smaller for the former than for the latter. The present data in acetone also exhibit an upswing with decreasing M_w for small M_w. This sharp increase in A_2 is similar to its behavior as observed for a-PMMA in acetone and also observed previously[2] for a-PS in toluene at 15.0 °C. Thus this behavior of A_2 for i-PMMA may be regarded as arising

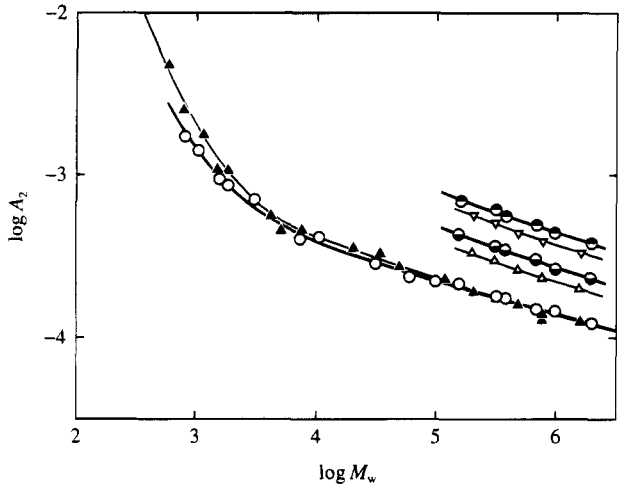

Figure 2. Double-logarithmic plots of A_2 against M_w for i-PMMA and a-PMMA: (○) i-PMMA in acetone at 25.0 °C; (●) i-PMMA in chloroform at 25.0 °C; (◒) i-PMMA in nitroethane at 30.0 °C; (▲) a-PMMA in acetone at 25.0 °C (previous data);[3] (▽) a-PMMA in chloroform at 25.0 °C (previous data);[3] (△) a-PMMA in nitroethane at 30.0 °C (previous data).[3] The solid curves connect the data points smoothly.

from the effect of chain ends as in the cases of a-PMMA and a-PS. The difference in A_2 between i- and a-PMMAs for $M_w \lesssim 2 \times 10^3$ may probably be due to that in the chemical structure at one of the chain ends between the i- and a-PMMA samples used. (Note that the i- and a-PMMA samples have a *tert*-butyl group and a hydrogen atom, respectively, at the initiating chain end, while both of them have a hydrogen atom at the other end.)

Discussion

HW Theory. For convenience, we begin by giving a brief description of the Yamakawa HW theory[4] of A_2. It considers the effect of chain ends on the basis of the HW touched-bead model (with excluded volume). It is such that $n + 1$ beads are arrayed with spacing a between them along the contour of total length $L = na$, where the $n - 1$ intermediate beads are identical and the two end beads are different from the intermediate ones and also from each other in species. Identical excluded-volume interactions are expressed in terms of the conventional binary-cluster integral β, while two kinds of effective excess binary-cluster integrals, β_1 and β_2, are necessary to express interactions between unlike (and like end) beads, β_1 being associated with one end bead and β_2 with two end ones. The HW model itself[5,6] is defined in terms of the three basic model parameters: the constant differential-geometrical curvature κ_0 and torsion τ_0 of its characteristic helix and the static stiffness parameter λ^{-1}.

According to the theory,[4] A_2 in general may be written in the form

$$A_2 = A_2^{(HW)} + A_2^{(E)} \tag{3}$$

where $A_2^{(HW)}$ is that part of A_2 without the effect of chain ends which vanishes at the definite temperature Θ independent of M, or A_2 for the (fictitious) chain composed of $n + 1$ identical beads, and $A_2^{(E)}$ represents the contribution of the effect of chain ends to A_2. The first term $A_2^{(HW)}$ may be written as

$$A_2^{(HW)} = (N_A c_\infty^{3/2} L^2 B/2M^2)h \tag{4}$$

where N_A is Avogadro's constant and the constant c_∞ and the excluded-volume strength B are given by

$$c_\infty = \lim_{\lambda L \to \infty} (6\lambda \langle S^2 \rangle_0 / L) = \frac{4 + (\lambda^{-1}\tau_0)^2}{4 + (\lambda^{-1}\kappa_0)^2 + (\lambda^{-1}\tau_0)^2} \tag{5}$$

and

$$B = \beta / a^2 c_\infty^{3/2} \tag{6}$$

The h function is given by

$$h(\hat{z}) = (1 + 7.74\hat{z} + 52.3\hat{z}^{27/10})^{-10/27} \tag{7}$$

with

$$\hat{z} = \tilde{\tilde{z}} / \alpha_S^3 \tag{8}$$

In eq 8, $\tilde{\tilde{z}}$ is the intermolecular scaled excluded-volume parameter defined by

$$\tilde{\tilde{z}} = [Q(\lambda L)/2.865]z \tag{9}$$

where the conventional excluded-volume parameter z is defined by

$$z = (3/2\pi)^{3/2}(\lambda B)(\lambda L)^{1/2} \tag{10}$$

and Q is a function only of λL for ordinary flexible polymers and given by eq 19 of ref 4 for $\lambda L \gtrsim 1$.

In the YSS theory,[17-19] α_S^2 ($= \langle S^2 \rangle / \langle S^2 \rangle_0$) is assumed to be a function only of the intramolecular scaled excluded-volume parameter $\tilde{z}$ defined by

$$\tilde{z} = (3/4)K(\lambda L)z \tag{11}$$

where K is a function only of λL and given by eq 9 of ref 4, and the Domb–Barrett equation[25] for α_S^2 is adopted with $\tilde{z}$ in place of z,

$$\alpha_S^2 = [1 + 10\tilde{z} + (70\pi/9 + 10/3)\tilde{z}^2 + 8\pi^{3/2}\tilde{z}^3]^{2/15} \times [0.933 + 0.067\exp(-0.85\tilde{z} - 1.39\tilde{z}^2)] \tag{12}$$

Thus, note that h is a function of $\tilde{z}$ and $\tilde{\tilde{z}}$ and that eq 4 for $A_2^{(HW)}$ is valid for $\lambda L \gtrsim 1$, and we may put $h = 1$ approximately for $\lambda L \lesssim 1$. Recall that L is related to M by the equation

$$L = M/M_L \tag{13}$$

with M_L the shift factor as defined as the molecular weight per unit contour length.

Now the second term $A_2^{(E)}$ in eq 3 may be written in the form

$$A_2^{(E)} = a_1 M^{-1} + a_2 M^{-2} \tag{14}$$

where

$$a_1 = 2N_A\beta_1/M_0$$

$$a_2 = 2N_A\Delta\beta_2 \tag{15}$$

with M_0 the molecular weight of the bead and with

$$\Delta\beta_2 = \beta_2 - 2\beta_1 \tag{16}$$

The effective excess binary-cluster integrals β_1 and β_2 are explicitly defined in eqs 22 of ref 4.

Effects of Chain Ends. We analyze the data for A_2 in acetone at 25.0 °C in Table 2 by the use of the theory above to first examine the effect of chain ends, as done previously[2,3] for a-PS and a-PMMA, for convenience. In Figure 3, the values of $A_2^{(E)} M_w$ are plotted against M_w^{-1}

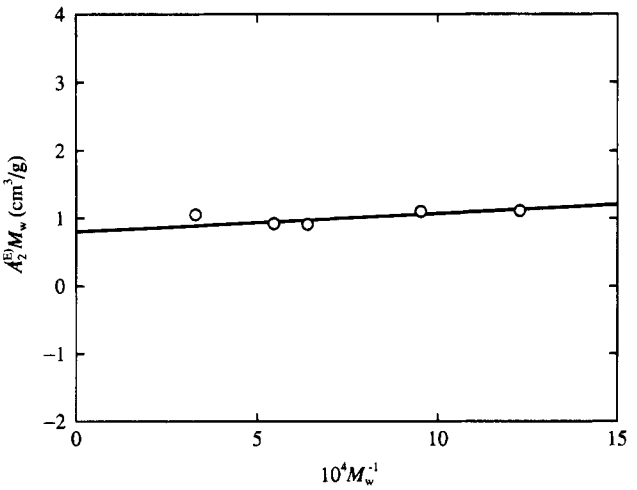

Figure 3. Plots of $A_2^{(E)}M_w$ against M_w^{-1} for i-PMMA in acetone at 25.0 °C.

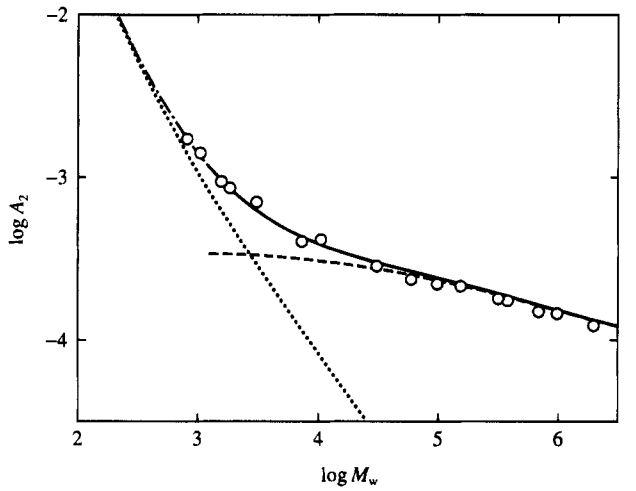

Figure 4. Comparison between the theoretical and observed values of A_2 as a function of M_w for i-PMMA in acetone at 25.0 °C. The solid and chain curves represent the theoretical values of A_2, and the dashed and dotted curves, those of $A_2^{(HW)}$ and $A_2^{(E)}$, respectively (see the text).

on the basis of eq 14 for the samples with $M_w \lesssim 3.1 \times 10^3$ in order to determine a_1 and a_2 (and hence β_1 and β_2) from the intercept and slope, respectively. Here, we have obtained the values of $A_2^{(E)}$ by subtracting $A_2^{(HW)}$ from A_2, where we have calculated $A_2^{(HW)}$ for each sample from eqs 4−13 (assuming that $h = 1$) with the values of the HW model parameters previously[8] determined from $\langle S^2\rangle_\Theta$, i.e., $\lambda^{-1}\kappa_0 = 2.5$, $\lambda^{-1}\tau_0 = 1.3$, $\lambda^{-1} = 38.0$ Å, and $M_L = 32.5$ Å^{-1}, and the value of B (or λB) determined[12] from α_S, i.e., $\lambda B = 0.10$.

It is seen that the data points can be fitted by a straight line. The result confirms the validity of eq 14, which predicts that the upswing of A_2 for small M arises from the effect of chain ends. From the straight line, a_1 and a_2 are found to be 0.80 cm^3/g and 270 cm^3/mol, respectively, with the uncertainties of ±12 and ±37%. Then, β_1 and β_2 are determined to be 66 and 360 Å^3, respectively, in acetone at 25.0 °C, from eqs 15 and 16 with the above values of a_1 and a_2 by taking the repeat unit of the chain as a single bead ($M_0 = 100$). These values of β_1 and β_2 are comparable to those obtained for a-PMMA in the same solvent.[3]

In Figure 4, the theoretical values of A_2 calculated with the values of all the parameters determined above

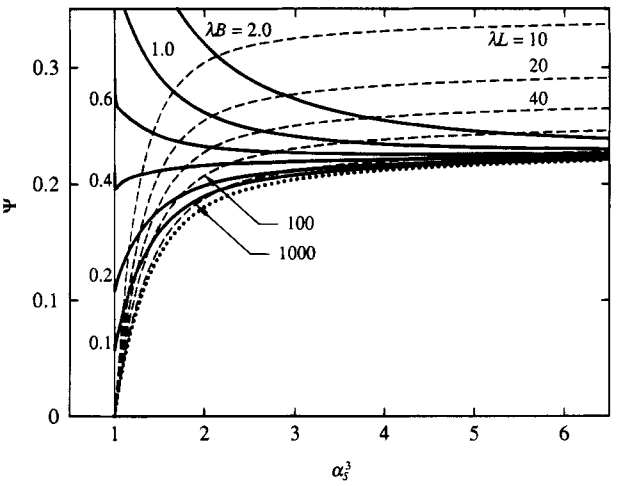

Figure 5. Plots of the theoretical Ψ against α_S^3 for i-PMMA. The solid and dashed curves represent the values at fixed λB and λL, respectively. The dotted curve represents the two-parameter-theory values.

are compared with the observed ones for the acetone solutions. Here, the solid curve represents the complete theoretical values, while the chain curve represents the values calculated with $h = 1$ for $\lambda L \lesssim 1$. The dashed and dotted curves indicate the calculated contributions of $A_2^{(HW)}$ and $A_2^{(E)}$ to A_2, respectively, in this system. There is seen to be good agreement between theory and experiment, although, strictly, the theoretical values seem to be slightly larger than the obesrved ones for $M_w \gtrsim 10^5$. It is also seen that the contribution of $A_2^{(E)}$ to A_2, i.e., the effect of chain ends, remains significant at least up to $M_w \simeq 10^5$. This finding is consistent with the previous results[2,3] for a-PS in toluene at 15.0 °C and for a-PMMA in acetone at 25.0 °C.

Interpenetration Function. We proceed to examine the effect of chain stiffness on the interpenetration function Ψ for i-PMMA in comparison with the previous results[3] for a-PMMA. Before making such a comparison between the observed results for i- and a-PMMAs, it is convenient to present the theoretical results for Ψ for the two polymers and discuss the predicted difference between them. As is evident from its original physical meaning,[7] the true interpenetration function Ψ without the effect of chain ends is defined by

$$\Psi = A_2^{(HW)}M^2/4\pi^{3/2}N_A\langle S^2\rangle^{3/2} \tag{17}$$

and it is given from eqs 4 and 17 by

$$\Psi = (6\lambda\langle S^2\rangle_0/c_\infty L)^{-3/2}(z/\alpha_S{}^3)h \tag{18}$$

In Figure 5 are shown values of Ψ for i-PMMA calculated from eq 18 with eqs 5−12 and eq 1 of ref 4 for $\langle S^2\rangle_0$ with the values of the parameters given above. The corresponding values for a-PMMA similarly calculated (see ref 3) are shown in Figure 6 (see also Figure 11 of ref 3). In these figures, the solid curves represent the values for the case in which λL (or M) is changed at fixed λB, while the dashed curves represent the values for the case in which λB is changed at fixed λL (or M), where the left end of each solid curve at $\alpha_S{}^3 = 1$ corresponds to $\lambda L = 1$. The dotted curve represents the two-parameter theory (coil-limiting) values calculated from[1-4]

$$\Psi = (z/\alpha_S{}^3)h \tag{19}$$

with $\tilde{z} = \tilde{z} = z$.

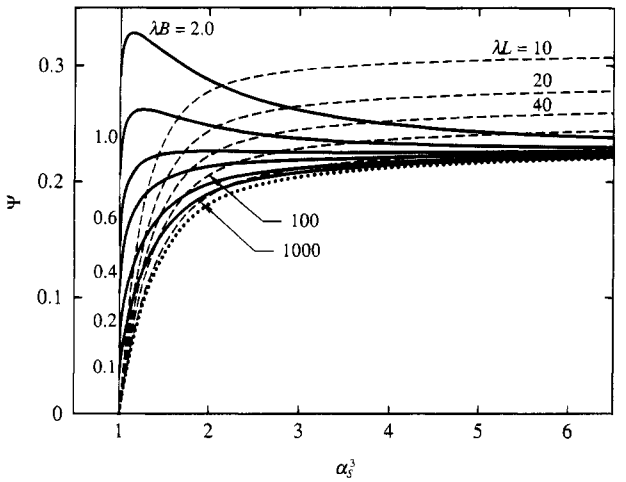

Figure 6. Plots of the theoretical Ψ against α_S^3 for a-PMMA. The solid and dashed curves represent the values at fixed λB and λL, respectively. The dotted curve represents the two-parameter-theory values.

It is seen from Figures 5 and 6 that for finite λB and λL, Ψ always deviates upward from the two-parameter-theory prediction, which is obtained as the asymptotic limit of $\lambda B \to 0$ or $\lambda L \to \infty$, for both i-PMMA and a-PMMA. However, there is a significant difference between the theoretical values for the two polymers. That is, as α_S^3 is decreased for small α_S^3 close to unity, for i-PMMA Ψ at fixed λB increases monotonically or after passing through a minimum while for a-PMMA it decreases monotonically or after passing through a maximum toward a finite value at $\lambda L = 1$. This difference is similar to that between the theoretical results for a-PS and a-PMMA[3] and may be explained by considering the large differences in chain stiffness and local chain conformation between the two PMMAs, which are reflected in the molecular weight dependence of $\langle S^2\rangle_0$ and $\langle S^2\rangle$.

Now we make a comparison between the observed results for i-PMMA and a-PMMA. We define as before[2] the *apparent* interpenetration function Ψ_{ap} from the whole A_2 with the contribution $A_2^{(E)}$ of the effect of chain ends by the equation

$$\Psi_{ap} = A_2 M^2/4\pi^{3/2} N_A \langle S^2\rangle^{3/2} \qquad (20)$$

In Table 6 are listed the values of Ψ and Ψ_{ap} for i-PMMA in acetone at 25.0 °C and those of Ψ in chloroform at 25.0 °C and in nitroethane at 30.0 °C, along with those of α_S^3. Here, the values of α_S^3 in acetone and in chloroform have been reproduced from ref 12 except for the sample iMMc16. In the calculation of α_S^3 in nitroethane, we have used the values of $\langle S^2\rangle_\Theta^{1/2}$ given in Table 4 of ref 8 and Table 3 of ref 12. We have calculated Ψ and Ψ_{ap} from eqs 17 and 20, respectively, with eq 3 with the values of M_w, A_2, and $\langle S^2\rangle^{1/2}$ in Tables 2–4. For the acetone solutions, we have obtained the values of $A_2^{(HW)}$ from A_2 by subtraction of $A_2^{(E)}$ calculated from eq 14 with the above values of a_1 and a_2. Since $A_2^{(E)}$ is negligibly small for $M_w \gtrsim 10^5$, Ψ (=Ψ_{ap}) for i-PMMA in nitroethane and in chloroform may be directly calculated from eq 20 with the respective experimental values of A_2. In fact, from a comparison between Ψ and Ψ_{ap} for i-PMMA in acetone, the contribution of $A_2^{(E)}$ to Ψ_{ap} is seen to be negligibly small in the ordinary range of M_w, i.e., for $M_w \gtrsim 1.5 \times 10^5$, but become progressively large as M_w is decreased.

Table 6. Values of Ψ (Ψ_{ap}) and α_S^3 for Isotactic Oligo- and Poly(methyl methacrylate)s in Acetone at 25.0 °C, in Chloroform at 25.0 °C, and in Nitroethane at 30.0 °C

	acetone, 25.0 °C[a]		chloroform, 25.0 °C[a]		nitroethane, 30.0 °C	
sample	Ψ (Ψ_{ap})	α_S^3	Ψ	α_S^3	Ψ	α_S^3
iOM7	0.062 (0.324)	(1.0)				
iOM10	0.074 (0.260)	1.02				
iOM31	0.069 (0.118)	1.08				
iOM71	0.071 (0.100)	1.02				
iMM1	0.090 (0.111)	1.15				
iMM3	0.108 (0.119)	1.21				
iMMc16	0.139 (0.142)	(1.55)[b]	0.260	(2.80)[b]	0.209	(1.97)[b]
iMMc30	0.152 (0.154)	1.70	0.248	3.75	0.226	2.35
iMMc40	0.160 (0.162)	1.68	0.237	3.78	0.216	2.42
iMMc70	0.169 (0.170)	1.91	0.236	4.61	0.229	2.79
iMMc90	0.184 (0.185)	2.08	0.229	5.06	0.219	3.24
iMMc190	0.188 (0.188)	2.46	0.234	6.13	0.220	3.78

[a] The values of α_S^3 have been reproduced from ref 12 with permission except for iMMc16 (present work). [b] The values of α_S^3 (in parentheses) have been calculated with the value 0.0934 Å^2 of $(\langle S^2\rangle_\Theta/M_w)_\infty$.[8,12]

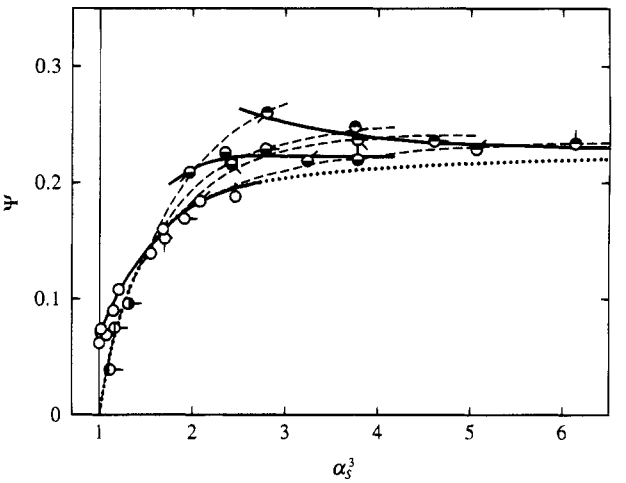

Figure 7. Plots of Ψ against α_S^3 for i-PMMA: (◑) in acetonitrile at 55.0 °C; ( ) in acetonitrile at 45.0 °C; (◐) in acetonitrile at 35.0 °C. The other types of circles have the same meaning as in Figure 2. Various directions of pips indicate different values of M_w of the six highest-molecular-weight samples: pip up, iMMc190; pip right-up, iMMc90; pip right, iMMc70; pip right-down, iMMc40; pip down, iMMc30; pip left-down, iMMc16. The solid and dashed curves connect smoothly the data points at fixed B (solvent condition) and M_w, respectively. The dotted curve represents the two-parameter-theory values.

All the data for Ψ thus determined are plotted against α_S^3 in Figure 7. It also includes the results for the acetonitrile solutions at the three temperatures higher than Θ, which have been calculated from eq 20 with the values of A_2 and $\langle S^2\rangle^{1/2}$ in Table 5 and with $M_w = 6.88 \times 10^5$ in Table 2. In the figure, various types of circles indicate different solvent conditions (different excluded-volume strengths B) and various directions of pips attached to them indicate different values of M_w of the six highest-molecular-weight samples. The solid curves connect smoothly the data points for different M_w at fixed B, while for those six samples the dashed curves connect smoothly the data points for different B at fixed M_w. In Figure 8, the previous results for a-PMMA in the same solvents as in Figure 7 have been reproduced from ref 3, for comparison. The symbols and curves have the same meaning as those in Figure 7.

As seen from Figure 7, the present results for i-PMMA again indicate that Ψ as a function of α_S^3 depends

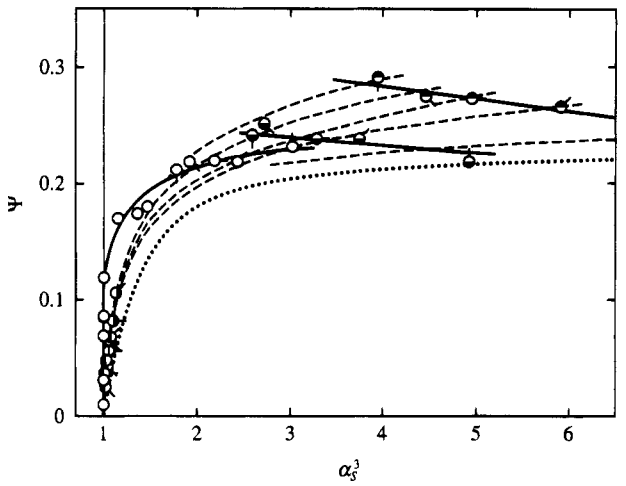

Figure 8. Plots of Ψ against α_S^3 for a-PMMA: (○) in acetone at 25.0 °C; (◓) in chloroform at 25.0 °C; (◒) in nitroethane at 30.0 °C; (◑) in acetonitrile at 55.0 °C; ( ) in acetonitrile at 50.0 °C; (◐) in acetonitrile at 47.0 °C. Various directions of pips indicate different values of M_w of the five highest-molecular-weight samples: pip up, $M_w = 1.58 \times 10^6$; pip right-up, 7.65×10^5; pip right, 4.82×10^5; pip right-down, 3.12×10^5; pip down, 2.04×10^5. The solid and dashed curves connect smoothly the data points at fixed B (solvent condition) and M_w, respectively. The dotted curve represents the two-parameter-theory values. Reproduced with permission from ref 3.

separately on M_w and on B, deviating appreciably upward from the two-parameter-theory prediction except for those in acetone for $M_w \geq 1.55 \times 10^5$ and in acetonitrile for $M_w = 6.88 \times 10^5$. For the acetone solutions, the data points closely follow the dotted curve for $M_w \geq 1.55 \times 10^5$, but they deviate upward from the latter for smaller M_w and follow the curve reaching a finite value of Ψ at $\alpha_S^3 = 1$. These results are in good agreement with the theoretical prediction shown in Figure 5.

From a comparison between the results in Figures 7 and 8, there is seen to be a remarkable difference in the behavior of Ψ between i-PMMA and a-PMMA. The data points for i-PMMA in each solvent (at fixed B) deviate less significantly from the dotted curve than those for a-PMMA in the same solvent. This difference can be explained as arising from that in the value of λB. As reported previously,[12,13] the values of λB for i-PMMA and a-PMMA are 0.55 and 1.15, respectively, in chloroform at 25.0 °C and 0.10 and 0.22, respectively, in acetone at 25.0 °C. A similar determination of λB for i-PMMA in nitroethane at 30.0 °C from the present data for α_S in Table 6 yields its value 0.24, while the corresponding value for a-PMMA in the same solvent is 0.52.[13] (We note that the values of β per repeat unit are the same, i.e., 28 Å^3 for i-PMMA and a-PMMA in nitroethane at 30.0 °C, confirming the previous finding that β is independent of the stereochemical structure of the polymer chain.) If we compare the results for i- and a-PMMAs in the solvent condition of similar values of λB, i.e., the results for i-PMMA in chloroform with those for a-PMMA in nitroethane and the results for i-PMMA in nitroethane with those for a-PMMA in acetone, then we find that the data points for the two polymers almost coincide with each other in the range of α_S^3 studied. This is consistent with the theoretical prediction. In fact, the solid curves for i-PMMA and a-PMMA at the same λB in Figures 5 and 6 also agree virtually with each other for $\alpha_S^3 \gtrsim 2$ when $\lambda B \leq 0.6$, although they split for smaller α_S^3. Unfortunately, the split in the range of small α_S^3 cannot be confirmed by the present experiment, since small-angle X-ray scattering measurements cannot be carried out to determine $\langle S^2 \rangle$ of the PMMA chain in chloroform and in nitroethane.

As for the above finding that Ψ for i-PMMA and a-PMMA in the same solvent exhibits the different dependence on α_S^3 despite the fact that they have the same value of β, it may be regarded as arising from the differences in chain stiffness and local chain conformation between the two polymers through λB and $\langle S^2 \rangle$. The theoretical results shown in Figures 5 and 6 indicate that the effects on $\langle S^2 \rangle$ become progressively significant with decreasing α_S^3.

Conclusion

In this work, we have determined A_2 from light scattering measurements for i-PMMA in acetone, in chloroform, and in nitroethane over a wide range of M_w, including the oligomer region. It has been found that A_2 in acetone at 25.0 °C increases steeply with decreasing M_w for $M_w \lesssim 2.0 \times 10^3$. This result may be quantitatively explained as before[2,3] by the Yamakawa theory[4] that takes account of the effect of chain ends. The analysis of these data for A_2 in acetone gives reasonable values of the effective excess binary-cluster integrals β_1 and β_2 associated with the chain end beads, and shows that the effect of chain ends on A_2, i.e., $A_2^{(E)}$, remains appreciable even for rather large M_w, as in the cases of a-PS[2] and a-PMMA.[3]

As for the interpenetration function Ψ, it has been found that the true Ψ without the effect of chain ends as a function of α_S^3 deviates significantly upward from the two-parameter-theory prediction except for the data in acetone for $M_w \gtrsim 10^5$. All the observed salient features of the behavior of Ψ as a function of α_S^3 for i-PMMA are qualitatively in good agreement with those previously found for a-PS[1,2] and for a-PMMA.[3] When a comparison is made between the results for i-PMMA and a-PMMA in the same solvent, the deviation of the observed Ψ from the two-parameter-theory prediction is less significant for the former than for the latter despite the fact that the values of β for them are close to each other. On the other hand, when such a comparison is made between the results for i-PMMA and a-PMMA in the solvent condition of similar values of λB, the data points for the two polymers almost coincide with each other in the range of relatively large α_S^3 studied. All these results for Ψ as a function of α_S^3 for the two PMMAs may be rather satisfactorily explained by the Yamakawa theory[4] that takes account of the effect of chain stiffness. In particular, it predicts that the values of Ψ for i-PMMA and a-PMMA with the same λB are virtually identical with each other for large α_S^3 in agreement with the observed results, although they are different for small α_S^3. These experimental and theoretical results indicate that the chain stiffness and local chain conformation have significant effects on the behavior of Ψ through λB and $\langle S^2 \rangle$.

References and Notes

(1) Yamakawa, H.; Abe, F.; Einaga, Y. *Macromolecules* **1993**, *26*, 1898.
(2) Einaga, Y.; Abe, F.; Yamakawa, H. *Macromolecules* **1993**, *26*, 6243.
(3) Abe, F.; Einaga, Y.; Yamakawa, H. *Macromolecules* **1994**, *27*, 3262.
(4) Yamakawa, H. Macromolecules **1992**, *25*, 1912.
(5) Yamakawa, H. *Annu. Rev. Phys. Chem.* **1984**, *35*, 23.

(6) Yamakawa, H. In *Molecular Conformation and Dynamics of Macromolecules in Condensed Systems*; Nagasawa, M., Ed.; Elsevier: Amsterdam, 1988; p 21.
(7) Yamakawa, H. *Modern Theory of Polymer Solutions*; Harper & Row: New York, 1971.
(8) Kamijo, M.; Sawatari, N.; Konishi, T.; Yoshizaki, T.; Yamakawa, H. *Macromolecules* **1994**, *27*, 5697.
(9) Horita, K.; Yoshizaki, T.; Hayashi, H.; Yamakawa, H. *Macromolecules* **1994**, *27*, 6492.
(10) Sawatari, N.; Konishi, T.; Yoshizaki, T.; Yamakawa, H. *Macromolecules* **1995**, *28*, 1089.
(11) Takaeda, Y.; Yoshizaki, T.; Yamakawa, H. *Macromolecules*, in press.
(12) Kamijo, M.; Abe, F.; Einaga, Y.; Yamakawa, H. *Macromolecules* **1995**, *28*, 1095.
(13) Abe, F.; Horita, K.; Einaga, Y.; Yamakawa, H. *Macromolecules* **1994**, *27*, 725.
(14) Abe, F.; Einaga, Y.; Yoshizaki, T.; Yamakawa, H. *Macromolecules* **1993**, *26*, 1884.
(15) Abe, F.; Einaga, Y.; Yamakawa, H. *Macromolecules* **1993**, *26*, 1891.
(16) Horita, K.; Abe, F.; Einaga, Y.; Yamakawa, H. *Macromolecules* **1993**, *26*, 5067.
(17) Yamakawa, H.; Stockmayer, W. H. *J. Chem. Phys.* **1972**, *57*, 2843.
(18) Yamakawa, H.; Shimada, J. *J. Chem. Phys.* **1985**, *83*, 2607.
(19) Shimada, J.; Yamakawa, H. *J. Chem. Phys.* **1986**, *85*, 591.
(20) Rubingh, D. N.; Yu, H. *Macromolecules* **1976**, *9*, 681.
(21) Einaga, Y.; Abe, F.; Yamakawa, H. *J. Phys. Chem.* **1992**, *96*, 3948.
(22) Berry, G. C. *J. Chem. Phys.* **1966**, *44*, 4550.
(23) Bawn, C. E. H.; Freeman, R. F. J.; Kamalidin, A. R. *Trans. Faraday Soc.* **1950**, *46*, 862.
(24) Norisuye, T.; Fujita, H. *ChemTracts: Macromol. Chem.* **1991**, *2*, 293.
(25) Domb, C.; Barrett, A. J. *Polymer* **1976**, *17*, 179.

MA946530V